ELSEVIER

International Journal of Solids and Structures 41 (2004) 2235–2257

INTERNATIONAL JOURNAL OF SOLIDS and STRUCTURES

www.elsevier.com/locate/ijsolstr

Semi-analytical solution for nonlinear vibration of laminated FGM plates with geometric imperfections

S. Kitipornchai [a,*], J. Yang [b,*], K.M. Liew [c,d]

[a] Department of Building and Construction, City University of Hong Kong, Tat Chee Avenue, Kowloon, Hong Kong
[b] Department of Civil Engineering, University of Queensland, St. Lucia, Brisbane 4072, Qld, Australia
[c] Nanyang Centre for Supercomputing and Visualisation, Nanyang Technological University, Nanyang Avenue, Singapore 639798, Singapore
[d] School of Mechanical and Production Engineering, Nanyang Technological University, Nanyang Avenue, Singapore 639798, Singapore

Received 14 December 2003; received in revised form 14 December 2003

Abstract

This paper investigates the nonlinear vibration of imperfect shear deformable laminated rectangular plates comprising a homogeneous substrate and two layers of functionally graded materials (FGMs). A theoretical formulation based on Reddy's higher-order shear deformation plate theory is presented in terms of deflection, mid-plane rotations, and the stress function. A semi-analytical method, which makes use of the one-dimensional differential quadrature method, the Galerkin technique, and an iteration process, is used to obtain the vibration frequencies for plates with various boundary conditions. Material properties are assumed to be temperature-dependent. Special attention is given to the effects of sine type imperfection, localized imperfection, and global imperfection on linear and nonlinear vibration behavior. Numerical results are presented in both dimensionless tabular and graphical forms for laminated plates with graded silicon nitride/stainless steel layers. It is shown that the vibration frequencies are very much dependent on the vibration amplitude and the imperfection mode and its magnitude. While most of the imperfect laminated plates show the well-known hard-spring vibration, those with free edges can display soft-spring vibration behavior at certain imperfection levels. The influences of material composition, temperature-dependence of material properties and side-to-thickness ratio are also discussed.

Keywords: Nonlinear vibration; Functionally gradient material; Laminated plate; Geometric imperfection; Higher-order shear deformation plate theory

1. Introduction

Numerous studies of the nonlinear vibration of isotropic and composite plate structures have been conducted with various theoretical models and solution approaches (Sathyamoorthy, 1987), most of which

* Corresponding authors. Tel.: +852-2788-8028; fax: +852-2788-7612 (S. Kitipornchai), Tel.: +61-733-653-912; fax: +61-733-654-599 (J. Yang).
E-mail addresses: bcskit@cityu.edu.hk (S. Kitipornchai), jie.yang@uq.edu.au (J. Yang).

0020-7683/$ - see front matter © 2004 Elsevier Ltd. All rights reserved.
doi:10.1016/j.ijsolstr.2003.12.019

are based on the assumption that the plates are perfect in shape. In practice, however, these structures can possess globally or locally distributed, small and unavoidable initial geometric imperfections (namely, deviations between the actual shape and the intended shape) during the fabrication process. As revealed by experimental results (Yamaki et al., 1983), these imperfections can have pronounced and complicated effects on the linear and nonlinear dynamic responses of plates in some cases. There have been quite a few investigations of the dynamics of imperfect, isotropic, homogeneous, thin, and moderately thick plates (see, Celep, 1976, 1980; Hui, 1983; Hui and Leissa, 1983; Lin and Chen, 1989; Chen and Lin, 1992). However, research into the nonlinear vibration of imperfect composite plates has been limited. Hui (1985) examined the influence of geometric imperfections on linear and large amplitude vibration of antisymmetrically laminated rectangular thin plates and reported that switch from a "hard-spring" character to "soft-spring" behavior may happen when the imperfection amplitude is of the order of half the plate thickness. By using the finite element method and polynomial functions to model the shape of imperfection modes, Kapania and Yang (1987) obtained the nonlinear vibration frequencies for isotropic and laminated thin plates with more general imperfections. Studies based on shear deformation plate theories include those by Chen and Yang (1993) and Bhimaraddi (1993) for antisymmetric angle-ply and symmetric cross-ply rectangular plates and the one by Bhimaraddi and Chandrashekhara (1993) for heated antisymmetric angle-ply rectangular plates. The above analyses found that for thicker isotropic plates, and even for some thin composite laminated plates, the effects of the transverse shear flexibility and rotary inertia become significant on the nonlinear dynamic response. Furthermore, the existence of a bending–stretching coupling effect in composites makes the vibration frequencies of some laminated plates very sensitive to geometric imperfections and initial stresses. With the exception of Kapania and Yang (1987), the aforementioned authors assumed that the imperfection mode was the same as the vibration mode, and presented results only for simple boundary conditions.

In the past few years, the use of functionally graded materials (FGMs) has gained intensive attention in many engineering applications, such as the aerospace, aircraft, automobile, and defense industries, and most recently the electronics and biomedical sectors (Ichikawa, 2000). A typical FGM, with a high bending–stretching coupling effect, is an inhomogeneous composite made from different phases of material constituents (usually ceramic and metal), with both the composition and material properties varying smoothly with spatial coordinates to take advantage of the desirable characteristics of each phase in order to achieve optimal distribution of material properties. It is often used in laminated plate structures and serves as a heat resistant layer of the metallic body. Several metallurgical techniques have been developed for the fabrication of FGMs. However, the complexity of the manufacturing process means that initial imperfections are inevitable.

A number of linear and nonlinear analyses of perfect, purely FGM structures have been conducted, notably those of Praveen and Reddy (1998), Noda (1999), Reddy (2000), Shen (2002a,b,c, 2003), Shen and Leung (2003), Vel and Batra (2002), and Yang and Shen (2002, 2003a). Several investigations of piezoelectric FGM laminated plates have also been reported (Reddy and Cheng, 2001; He et al., 2001; Liew et al., 2003). However, research work on imperfect FGM plates is scarce. Yang and Shen (2003b) made the only attempt to investigate the postbuckling behavior of imperfect FGM rectangular plates under transverse and in-plane loads. They used classical plate theory (CPT) and assumed that the geometric imperfection was the same as the buckling mode. As far as the authors are aware, no previous work has been done on the nonlinear dynamic behavior of imperfect FGM plates.

This paper aims to investigate the linear and nonlinear vibration behavior of imperfect, shear deformable FGM laminated rectangular plates in the framework of Reddy's higher-order shear deformation plate theory (Reddy, 1984). Attention is focused on the effects of different imperfection modes on the vibration characteristics of plates with temperature-dependent material properties and under general boundary conditions. Instead of assuming the imperfection mode to be the same as the vibration mode, a variety of sine type, localized type, and global type imperfections are considered. A semi-analytical approach, which

employs the differential quadrature, the Galerkin method, and the iteration procedure, is used to determine the vibration frequencies of the plate. Extensive numerical results for laminated plates with FGM layers made of silicon nitride and stainless steel are presented in both dimensionless tabular and graphical forms to show that their vibration behavior is highly sensitive to initial imperfections, especially the localized imperfection at the plate center, and that "soft-spring" vibration behavior can take place in imperfect FGM laminated plates with free edges.

2. Theoretical formulations

2.1. The plate model

Consider an imperfect laminated rectangular plate $[0 \leqslant X_1 \leqslant a, 0 \leqslant X_2 \leqslant b, -h/2 \leqslant X_3 \leqslant h/2]$ that consists of a homogeneous substrate of thickness h_c and two inhomogeneous FGM layers of the same layer thickness h_F. Both the top surface ($X_3 = h_c/2$) and the bottom surface ($X_3 = -h_c/2$) of the substrate are perfectly bonded to an FGM layer to form a symmetrically laminated plate structure, as shown in Fig. 1. The plate is designed such that the material at the two interfacial surfaces is the same in order to eliminate the property mismatch.

It is assumed that the FGM is made of a mixture of a ceramic phase (denoted by "c") and a metal phase (denoted by "m"), with the material composition varying smoothly along its thickness direction (i.e. in the X_3-axis) only. Its local effective material properties P_{eff} at a given point are then position dependent, and can be estimated through the homogenization technique that is based on the simple rule-of-mixture (Markworth and Saunders, 1995) as

$$P_{\text{eff}} = P_m + (P_c - P_m)V_c, \tag{1}$$

where the ceramic volume fraction V_c is described by

$$V_c = \begin{cases} \left(\frac{2X_3 - h_c}{2h_F}\right)^n & X_3 \geqslant h_c/2, \\ \left(-\frac{2X_3 + h_c}{2h_F}\right)^n & X_3 \leqslant -h_c/2, \end{cases} \tag{2a}$$

and the metal volume fraction is

$$V_m = 1 - V_c, \tag{2b}$$

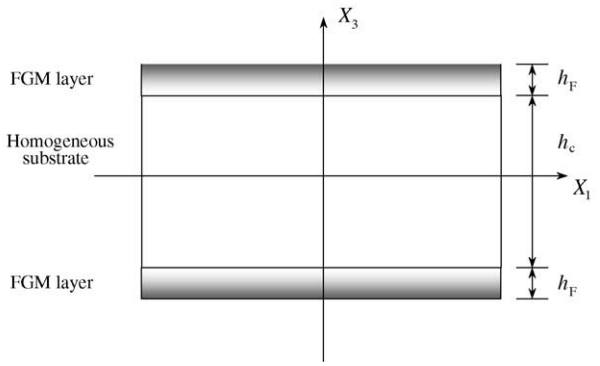

Fig. 1. The cross-section of a symmetrically laminated plate comprising FGM.

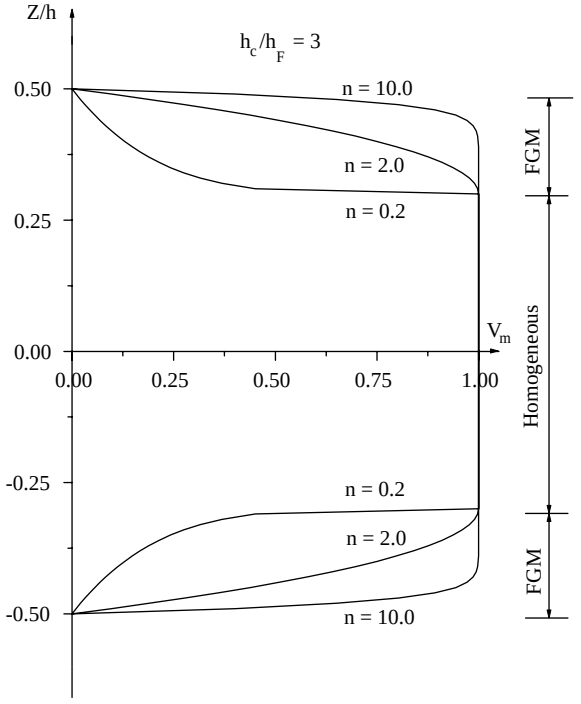

Fig. 2. Variation of volume fraction V_m in the thickness direction of the laminated plate.

where n is a non-negative volume fraction index and can be optimized to achieve the desired performance. It is evident from Eq. (2) that the outer surfaces of FGM layers $X_3 = \pm(0.5h_c + h_F)$ are purely ceramic, while the inner surfaces $X_3 = \pm 0.5h_c$ are fully metallic. Variation of volume fraction V_m in the thickness direction of a typical laminated plate is shown in Fig. 2.

This study only considers transverse initial geometric imperfection $\overline{W}^*$ in a stress-free state. The imperfect shape can be of an arbitrary type, but the Wadee (2000) one-dimensional imperfection model for struts is extended to describe the various possible imperfection modes, which take the form of the products of trigonometric functions and hyperbolic functions in the X_1–X_2 plane

$$\overline{W}^* = \eta h \sec h[\delta_1(x_1 - \psi_1)] \cos[\mu_1 \pi(x_1 - \psi_1)] \sec h[\delta_2(x_2 - \psi_2)] \cos[\mu_2 \pi(x_2 - \psi_2)], \tag{3}$$

where $x_1 = X_1/a$, $x_2 = X_2/b$, η is the maximum dimensionless amplitude of the initially deflected geometry, δ_1 and δ_2 are the constants defining the localization degree of the imperfection that is symmetric about $x_1 = \psi_1$ and $x_2 = \psi_2$, and μ_1 and μ_2 are the half-wave numbers of the imperfection in X_1- and X_2-axis, respectively. This expression is capable of modeling a wide range of initial imperfection modes, including: (a) the sine type, when $\delta_1 = \delta_2 = 0$, $\mu_1 = \mu_2 = 1$, $\psi_1 = \psi_2 = 0.5$; (b) the localized type, when $\delta_1 \neq 0$, $\delta_2 \neq 0$; and (c) the global type, when $\delta_1 = \delta_2 = 0$, $\mu_1 \neq 1$ or $\mu_2 \neq 1$. A list of the imperfection modes that will be used in Section 4 is given in Table 1 where Cases G1, G2, and G3 are global imperfection modes while Cases L1, L2, L3, L4, and L5 are localized imperfection modes.

2.2. Governing equations

Let $\overline{U}_k$ ($k = 1, 2, 3$) denote the dynamic displacement components in the X_k direction, t the time. The displacement field of an arbitrary point within the plate domain is assumed, in accordance with Reddy's higher-order shear deformation plate theory, to be

Table 1
Imperfection modes

Sine type	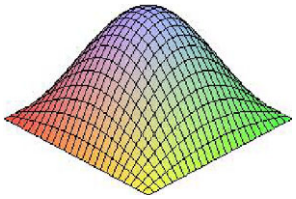	$\delta_1 = 0,\ \mu_1 = 1,\ \psi_1 = 0.5$ $\delta_2 = 0,\ \mu_2 = 1,\ \psi_2 = 0.5$	
Case G1	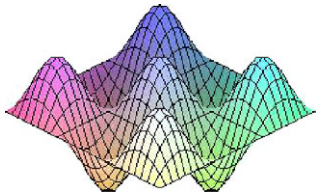	$\delta_1 = 0,\ \mu_1 = 3,\ \psi_1 = 0.5$ $\delta_2 = 0,\ \mu_2 = 3,\ \psi_2 = 0.5$	
Case G2	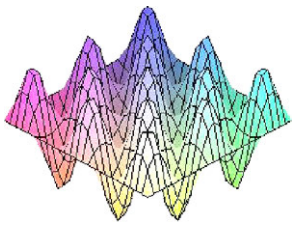	$\delta_1 = 0,\ \mu_1 = 5,\ \psi_1 = 0.5$ $\delta_2 = 0,\ \mu_2 = 5,\ \psi_2 = 0.5$	
Case G3	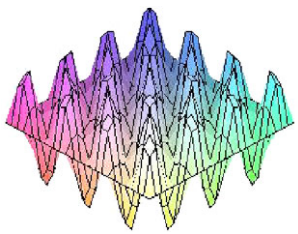	$\delta_1 = 0,\ \mu_1 = 7,\ \psi_1 = 0.5$ $\delta_2 = 0,\ \mu_2 = 7,\ \psi_2 = 0.5$	
Case L1	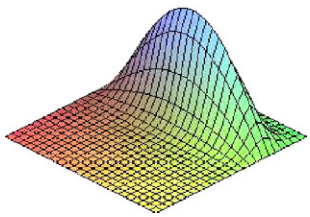	$\delta_1 = 15,\ \mu_1 = 2,\ \psi_1 = 0.25$ $\delta_2 = 0,\ \mu_2 = 1,\ \psi_2 = 0.5$	
Case L2	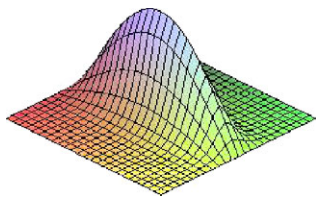	$\delta_1 = 15,\ \mu_1 = 2,\ \psi_1 = 0.5$ $\delta_2 = 0,\ \mu_2 = 1,\ \psi_2 = 0.5$	
Case L3	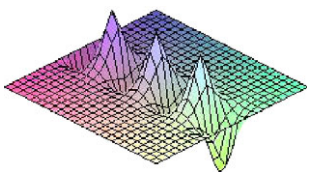	$\delta_1 = 15,\ \mu_1 = 2,\ \psi_1 = 0.5$ $\delta_2 = 0,\ \mu_2 = 3,\ \psi_2 = 0.5$	
Case L4	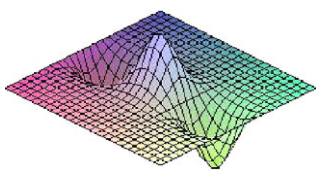	$\delta_1 = 15,\ \mu_1 = 2,\ \psi_1 = 0.5$ $\delta_2 = 0,\ \mu_2 = 5,\ \psi_2 = 0.5$	
Case L5	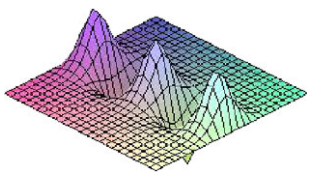	$\delta_1 = 15,\ \mu_1 = 2,\ \psi_1 = 0.5$ $\delta_2 = 0,\ \mu_2 = 7,\ \psi_2 = 0.5$	

$$\overline{U}_1 = \overline{U}(X,Y,t) + X_3\overline{\Psi}_1(X,Y,t) - c_1X_3^3\left(\overline{\Psi}_1(X,Y,t) + \frac{\partial\overline{U}_3}{\partial X_1}\right), \tag{4a}$$

$$\overline{U}_2 = \overline{V}(X,Y,t) + X_3\overline{\Psi}_2(X,Y,t) - c_1X_3^3\left(\overline{\Psi}_2(X,Y,t) + \frac{\partial\overline{U}_3}{\partial X_2}\right), \tag{4b}$$

$$\overline{U}_3 = \overline{W}(X,Y,t) + \overline{W}^*(X,Y), \tag{4c}$$

where $c_1 = 4/3h^2$, $(\overline{U},\overline{V},\overline{W})$ are the displacements of a point on the mid-plane, and $\overline{\Psi}_1$ and $\overline{\Psi}_2$ are the slope rotations in the X_1–X_3 and X_2–X_3 planes due to bending only.

As the in-plane displacements $\overline{U}_1$ and $\overline{U}_2$ are small compared to the transverse displacement $\overline{U}_3$ and the higher-order terms are negligible, the nonlinear strains of an imperfect plate are defined as

$$\begin{aligned}
&\varepsilon_1 = \varepsilon_1^{(0)} + X_3\left[\varepsilon_1^{(1)} + X_3^2\varepsilon_1^{(3)}\right], \qquad \varepsilon_2 = \varepsilon_2^{(0)} + X_3\left[\varepsilon_2^{(1)} + X_3^2\varepsilon_2^{(3)}\right],\\
&\varepsilon_6 = \varepsilon_6^{(0)} + X_3\left[\varepsilon_6^{(1)} + X_3^2\varepsilon_6^{(3)}\right], \qquad \varepsilon_4 = \varepsilon_4^{(0)} + X_3^2\varepsilon_4^{(2)}, \qquad \varepsilon_5 = \varepsilon_5^{(0)} + X_3^2\varepsilon_5^{(2)},
\end{aligned} \tag{5}$$

where

$$\begin{aligned}
\varepsilon_1^{(0)} &= \frac{\partial\overline{U}}{\partial X_1} + \frac{1}{2}\left(\frac{\partial\overline{W}}{\partial X_1}\right)^2 + \frac{\partial\overline{W}}{\partial X_1}\frac{\partial\overline{W}^*}{\partial X_1}, \quad \varepsilon_1^{(1)} = \frac{\partial\overline{\Psi}_1}{\partial X_1}, \quad \varepsilon_1^{(3)} = -c_1\left(\frac{\partial\overline{\Psi}_1}{\partial X_1} + \frac{\partial^2\overline{W}}{\partial X_1^2} + \frac{\partial^2\overline{W}^*}{\partial X_1^2}\right),\\
\varepsilon_2^{(0)} &= \frac{\partial\overline{U}}{\partial X_2} + \frac{1}{2}\left(\frac{\partial\overline{W}}{\partial X_2}\right)^2 + \frac{\partial\overline{W}}{\partial X_2}\frac{\partial\overline{W}^*}{\partial X_2}, \quad \varepsilon_2^{(1)} = \frac{\partial\overline{\Psi}_2}{\partial X_2}, \quad \varepsilon_2^{(3)} = -c_1\left(\frac{\partial\overline{\Psi}_2}{\partial X_2} + \frac{\partial^2\overline{W}}{\partial X_2^2} + \frac{\partial^2\overline{W}^*}{\partial X_2^2}\right),\\
\varepsilon_6^{(0)} &= \frac{\partial\overline{U}}{\partial X_2} + \frac{\partial\overline{V}}{\partial X_1} + \frac{\partial\overline{W}}{\partial X_1}\frac{\partial\overline{W}}{\partial X_2} + \frac{\partial\overline{W}^*}{\partial X_1}\frac{\partial\overline{W}}{\partial X_2} + \frac{\partial\overline{W}}{\partial X_1}\frac{\partial\overline{W}^*}{\partial X_2},\\
\varepsilon_6^{(1)} &= \frac{\partial\overline{\Psi}_1}{\partial X_2} + \frac{\partial\overline{\Psi}_2}{\partial X_1}, \quad \varepsilon_6^{(3)} = -c_1\left(\frac{\partial\overline{\Psi}_1}{\partial X_2} + \frac{\partial\overline{\Psi}_2}{\partial X_1} + 2\frac{\partial^2\overline{W}}{\partial X_1\partial X_2} + 2\frac{\partial^2\overline{W}^*}{\partial X_1\partial X_2}\right),\\
\varepsilon_4^{(0)} &= \overline{\Psi}_2 + \frac{\partial\overline{W}}{\partial X_2} + \frac{\partial\overline{W}^*}{\partial X_2}, \quad \varepsilon_4^{(2)} = -3c_1\left(\overline{\Psi}_2 + \frac{\partial\overline{W}}{\partial X_2} + \frac{\partial\overline{W}^*}{\partial X_2}\right),\\
\varepsilon_5^{(0)} &= \overline{\Psi}_1 + \frac{\partial\overline{W}}{\partial X_1} + \frac{\partial\overline{W}^*}{\partial X_1}, \quad \varepsilon_5^{(2)} = -3c_1\left(\overline{\Psi}_1 + \frac{\partial\overline{W}}{\partial X_1} + \frac{\partial\overline{W}^*}{\partial X_1}\right).
\end{aligned} \tag{6}$$

Let $\overline{F}$ be the stress function that is related to the stress resultants by $\overline{N}_1 = \overline{F}_{,X_2X_2}$, $\overline{N}_2 = \overline{F}_{,X_1X_1}$, $\overline{N}_6 = -\overline{F}_{,X_1X_2}$, where a comma denotes partial differentiation with respect to the coordinates. The nonlinear governing equations can be derived as follows:

$$\begin{aligned}
&\frac{\partial\overline{Q}_1}{\partial X_1} + \frac{\partial\overline{Q}_2}{\partial X_2} - 3c_1\left(\frac{\partial\overline{R}_1}{\partial X_1} + \frac{\partial\overline{R}_2}{\partial X_2}\right) + c_1\left(\frac{\partial^2\overline{P}_1}{\partial X_1^2} + 2\frac{\partial^2\overline{P}_6}{\partial X_1\partial X_2} + \frac{\partial^2\overline{P}_2}{\partial X_2^2}\right) + \widetilde{L}(\overline{W}+\overline{W}^*,\overline{F})\\
&\quad = I_1\ddot{\overline{W}} + I_7'\left(\frac{\partial^2\ddot{\overline{W}}}{\partial X_1^2} + \frac{\partial^2\ddot{\overline{W}}}{\partial X_2^2}\right) + I_5'\left(\frac{\partial\ddot{\overline{\Psi}}_1}{\partial X_1} + \frac{\partial\ddot{\overline{\Psi}}_2}{\partial X_2}\right),
\end{aligned} \tag{7}$$

$$\frac{\partial\overline{M}_1}{\partial X_1} + \frac{\partial\overline{M}_6}{\partial X_2} - \overline{Q}_1 + 3c_1\overline{R}_1 - c_1\left(\frac{\partial\overline{P}_1}{\partial X_1} + \frac{\partial\overline{P}_6}{\partial X_2}\right) = I_3'\ddot{\overline{\Psi}}_1 - I_5'\frac{\partial\ddot{\overline{W}}}{\partial X_1}, \tag{8}$$

$$\frac{\partial\overline{M}_6}{\partial X_1} + \frac{\partial\overline{M}_2}{\partial X_2} - \overline{Q}_2 + 3c_1\overline{R}_2 - c_1\left(\frac{\partial\overline{P}_6}{\partial X_1} + \frac{\partial\overline{P}_2}{\partial X_2}\right) = I_3'\ddot{\overline{\Psi}}_2 - I_5'\frac{\partial\ddot{\overline{W}}}{\partial X_2}, \tag{9}$$

$$\frac{\partial^2 \varepsilon_1^{(0)}}{\partial X_2^2}+\frac{\partial^2 \varepsilon_2^{(0)}}{\partial X_1^2}-\frac{\partial^2 \varepsilon_6^{(0)}}{\partial X_1\,\partial X_2}=\left(\frac{\partial^2 \overline{W}}{\partial X_1\,\partial X_2}\right)^2-\frac{\partial^2 \overline{W}}{\partial X_1^2}\frac{\partial^2 \overline{W}}{\partial X_2^2}+2\frac{\partial^2 \overline{W}}{\partial X_1\,\partial X_2}\frac{\partial^2 \overline{W}^*}{\partial X_1\,\partial X_2}-\frac{\partial^2 \overline{W}}{\partial X_1^2}\frac{\partial^2 \overline{W}^*}{\partial X_2^2}-\frac{\partial^2 \overline{W}}{\partial X_2^2}\frac{\partial^2 \overline{W}^*}{\partial X_1^2}, \tag{10}$$

where $\widetilde{L}(,)=\frac{\partial^2}{\partial X_1^2}\frac{\partial^2}{\partial X_2^2}-2\frac{\partial^2}{\partial X_1\,\partial X_2}\frac{\partial^2}{\partial X_1\,\partial X_2}+\frac{\partial^2}{\partial X_2^2}\frac{\partial^2}{\partial X_1^2}$, a super dot implies differentiation with respect to time t, and

$$\begin{aligned}
&I_3'=\overline{I}_3-\overline{I}_2^2/I_1, \qquad I_5'=c_1(\overline{I}_5-I_4\overline{I}_2/I_1), \qquad I_7'=c_1^2(I_4^2/I_1-I_7),\\
&\overline{I}_2=I_2-c_1I_4, \qquad \overline{I}_3=I_3-2c_1I_5+c_1^2I_7, \qquad \overline{I}_5=I_5-c_1I_7,\\
&(I_1,I_2,I_3,I_4,I_5,I_7)=\sum_{k=1}^{N_L}\int_{X_3^{(k-1)}}^{X_3^{(k)}}\rho^{(k)}\left(1,X_3,X_3^2,X_3^3,X_3^4,X_3^6\right)\mathrm{d}X_3.
\end{aligned} \tag{11}$$

Stress resultants $\overline{N}_i$, moments $\overline{M}_i$, higher-order moments $\overline{P}_i$, transverse shear forces $\overline{Q}_i$ and their higher-order counterparts $\overline{R}_i$ are related to strains through a partial inverse relationship

$$\begin{Bmatrix}\varepsilon_i^{(0)}\\ \overline{M}_i\\ \overline{P}_i\end{Bmatrix}=\begin{bmatrix}A_{ij}^* & B_{ij}^* & E_{ij}^*\\ -B_{ji}^* & D_{ij}^* & F_{ji}^*\\ -E_{ji}^* & F_{ij}^* & H_{ij}^*\end{bmatrix}\begin{Bmatrix}\overline{N}_j\\ \varepsilon_j^{(1)}\\ \varepsilon_j^{(3)}\end{Bmatrix} \quad (i,j=1,2,6), \tag{12a}$$

$$\begin{Bmatrix}\overline{Q}_i\\ \overline{R}_i\end{Bmatrix}=\begin{bmatrix}A_{ij} & D_{ij}\\ D_{ij} & F_{ij}\end{bmatrix}\begin{Bmatrix}\varepsilon_j^{(0)}\\ \varepsilon_j^{(2)}\end{Bmatrix} \quad (i,j=4,5). \tag{12b}$$

The relations to determine the above reduced plate stiffness elements are available in open literature (see, for example, Shen, 2002a,b,c, 2003) and therefore are omitted for brevity.

A fully movable laminated plate that is either simply supported (S) or clamped (C) at both edges $X_2=0$, 1, and can be supported (S), clamped (C), or free (F) at the other edges is considered. The associated boundary conditions take the form

at $X_1=0$, a:

$$\text{Simply supported (S)}: \quad \overline{W}=\overline{M}_1=\overline{\Psi}_2=\overline{P}_1=\overline{N}_1=\overline{N}_6=0, \tag{13a}$$

$$\text{Clamped (C)}: \quad \overline{W}=\overline{\Psi}_1=\overline{\Psi}_2=\frac{\partial \overline{W}}{\partial X_1}=\overline{N}_1=\overline{N}_6=0, \tag{13b}$$

$$\text{Free (F)}: \quad \overline{Q}_1^*=\overline{M}_1=\overline{M}_6^*=\overline{P}_1=\overline{N}_1=\overline{N}_6=0; \tag{13c}$$

at $X_2=0$, b:

$$\text{Simply supported (S)}: \quad \overline{W}=\overline{M}_2=\overline{\Psi}_1=\overline{P}_2=\overline{N}_2=\overline{N}_6=0, \tag{14a}$$

$$\text{Clamped (C)}: \quad \overline{W}=\overline{M}_2=\overline{\Psi}_1=\frac{\partial \overline{W}}{\partial X_2}=\overline{N}_2=\overline{N}_6=0; \tag{14b}$$

where $\overline{Q}_1^*$ and $\overline{M}_6^*$ are the generalized transverse shear force and moment at $X_1=0$, 1. Their definitions are given by Reddy (1984).

2.3. Dimensionless governing equations

With the following dimensionless quantities,

$$x_1 = X_1/a, \qquad x_2 = X_2/b, \qquad \beta = a/b, \qquad (W, W^*) = (\overline{W}, \overline{W}^*)/(D_{11}^* D_{22}^* A_{11}^* A_{22}^*)^{1/4},$$
$$F = \overline{F}/(D_{11}^* D_{22}^*)^{1/2}, \qquad (\Psi_1, \Psi_2) = (\overline{\Psi}_1, \overline{\Psi}_2)a/(D_{11}^* D_{22}^* A_{11}^* A_{22}^*)^{1/4}, \tag{15}$$
$$(I_3^*, I_5^*, I_7^*) = (I_3', I_5', I_7')/I_1 a^2, \qquad \widehat{I}_5^* = I_3^* + I_5^*, \qquad \widehat{I}_7^* = I_7^* - I_5^*,$$

the mid-plane of the plate is normalized into a square domain $[0 \leqslant x_1 \leqslant 1, 0 \leqslant x_2 \leqslant 1]$, and the governing Eqs. (7)–(10) can be expressed in terms of W, Ψ_1, Ψ_2, and F as

$$\gamma_{110}\frac{\partial^4 W}{\partial x_1^4} + 2\gamma_{112}\beta^2\frac{\partial^4 W}{\partial x_1^2 \partial x_2^4} + \gamma_{114}\beta^4\frac{\partial^4 W}{\partial x_2^4} - \left(\gamma_{120}\frac{\partial^3 \Psi_1}{\partial x_1^3} + \gamma_{122}\beta^2\frac{\partial^3 \Psi_1}{\partial x_1 \partial x_2^2}\right)$$
$$- \beta\left(\gamma_{131}\frac{\partial^3 \Psi_2}{\partial x_1^2 \partial x_2} + \gamma_{133}\beta^2\frac{\partial^3 \Psi_2}{\partial x_2^3}\right) + \gamma_{14}\left(\gamma_{140}\frac{\partial^4 F}{\partial x_1^4} + \gamma_{142}\beta^2\frac{\partial^4 F}{\partial x_1^2 \partial x_2^2} + \gamma_{144}\beta^4\frac{\partial^4 F}{\partial x_2^4}\right)$$
$$= \gamma_{14}\beta^2 L(W + W^*, F) - \left[\ddot{W} + \widehat{I}_7^*\left(\frac{\partial^2 \ddot{W}}{\partial x_1^2} + \beta^2\frac{\partial^2 \ddot{W}}{\partial x_2^2}\right) + \widehat{I}_5^*\left(\frac{\partial \ddot{\Psi}_1}{\partial x_1} + \frac{\partial \ddot{\Psi}_2}{\partial x_2}\right)\right], \tag{16}$$

$$\gamma_{31}\frac{\partial W}{\partial x_1} + \gamma_{310}\frac{\partial^3 W}{\partial x_1^3} + \gamma_{312}\beta^2\frac{\partial^3 W}{\partial x_1 \partial x_2^2} + \left(\gamma_{31}\Psi_1 - \gamma_{320}\frac{\partial^2 \Psi_1}{\partial x_1^2} - \gamma_{322}\beta^2\frac{\partial^2 \Psi_1}{\partial x_2^2}\right) - \gamma_{331}\beta\frac{\partial^2 \Psi_2}{\partial x_1 \partial x_2}$$
$$+ \gamma_{14}\left(\gamma_{220}\frac{\partial^3 F}{\partial x_1^3} + \gamma_{222}\beta^2\frac{\partial^3 F}{\partial x_1 \partial x_2^2}\right) = -\left(I_3^*\ddot{\Psi}_1 - I_5^*\frac{\partial \ddot{W}}{\partial x_1}\right), \tag{17}$$

$$\beta\left(\gamma_{41}\frac{\partial W}{\partial x_2} + \gamma_{411}\frac{\partial^3 W}{\partial x_1^2 \partial x_2} + \gamma_{413}\beta^2\frac{\partial^3 W}{\partial x_2^3}\right) - \gamma_{331}\beta\frac{\partial^2 \Psi_1}{\partial x_1 \partial x_2} + \left(\gamma_{41}\Psi_2 - \gamma_{430}\frac{\partial^2 \Psi_2}{\partial x_1^2} - \gamma_{432}\beta^2\frac{\partial^2 \Psi_2}{\partial x_2^2}\right)$$
$$+ \gamma_{14}\beta\left(\gamma_{231}\frac{\partial^3 F}{\partial x_1^2 \partial x_2} + \gamma_{233}\beta^2\frac{\partial^3 F}{\partial x_2^3}\right) = -\left(I_3^*\ddot{\Psi}_2 - I_5^*\frac{\partial \ddot{W}}{\partial x_2}\right), \tag{18}$$

$$\frac{\partial^4 F}{\partial x_1^4} + \gamma_{212}\beta^2\frac{\partial^4 F}{\partial x_1^2 \partial x_2^2} + \gamma_{24}^2\beta^4\frac{\partial^4 F}{\partial x_2^4} + \gamma_{24}\left(\gamma_{220}\frac{\partial^3 \Psi_1}{\partial x^3} + \gamma_{222}\beta^2\frac{\partial^3 \Psi_1}{\partial x \partial x_2^2}\right) + \gamma_{24}\beta\left(\gamma_{231}\frac{\partial^3 \Psi_2}{\partial x_1^2 \partial x_2} + \gamma_{233}\beta^2\frac{\partial^3 \Psi_2}{\partial x_2^3}\right)$$
$$- \gamma_{24}\left(\gamma_{240}\frac{\partial^4 W}{\partial x_1^4} + \gamma_{242}\beta^2\frac{\partial^4 W}{\partial x_1^2 \partial x_2^2} + \gamma_{244}\beta^4\frac{\partial^4 W}{\partial x_2^4}\right) = -\frac{1}{2}\gamma_{24}\beta^2 L(W + 2W^*, W), \tag{19}$$

where $L(,) = \frac{\partial^2}{\partial x_1^2}\frac{\partial^2}{\partial x_2^2} - 2\frac{\partial^2}{\partial x_1 \partial x_2}\frac{\partial^2}{\partial x_1 \partial x_2} + \frac{\partial^2}{\partial x_1^2}\frac{\partial^2}{\partial x_2^2}$, and the coefficients γ_{ij} and γ_{ijk} are defined by Yang and Shen (2003c).

The boundary conditions (13) and (14) now become

at $x_1 = 0$, 1:

$$\text{Simply supported (S)}: \quad W = M_1 = \Psi_2 = P_1 = N_1 = N_6 = 0, \tag{20a}$$

$$\text{Clamped (C)}: \quad W = \Psi_1 = \Psi_2 = \frac{\partial W}{\partial x_1} = N_1 = N_6 = 0, \tag{20b}$$

$$\text{Free (F)}: \quad Q_1^* = M_1 = M_6^* = P_1 = N_1 = N_6 = 0; \tag{20c}$$

at $x_2 = 0$, 1:

$$\text{Simply supported (S)}: \quad W = M_2 = \Psi_1 = P_2 = N_2 = N_6 = 0, \tag{21a}$$

$$\text{Clamped (C)}: \quad W = M_2 = \Psi_1 = \frac{\partial W}{\partial x_2} = N_2 = N_6 = 0 \tag{21b}$$

in which

$$(M_1, M_2, P_1, P_2, M_6^*, Q_1^*) = (\overline{M}_1, \overline{M}_2, c_1\overline{P}_1, c_1\overline{P}_2, \overline{M}_6^*, \overline{Q}_1^* a)a^2/D_{11}^*(D_{11}^* D_{22}^* A_{11}^* A_{22}^*)^{1/4}. \tag{22}$$

3. Semi-analytical method

A semi-analytical approach that was proposed by Yang and Shen (2002, 2003a,c), together with an iterative algorithm, is used to study the nonlinear vibration of the imperfect laminated plate. The approach employs the one-dimensional differential quadrature rule and the Galerkin technique to establish a nonlinear eigenvalue system from which the nonlinear fundamental frequencies at given vibration amplitudes are determined through an iteration process.

Bellman (1973) proposed the differential quadrature method to solve linear and nonlinear differential equations, and it was later introduced to structural analysis by Jang et al. (1989), Bert and Malik (1996), Bert et al. (1993, 1998) and Liew et al. (2001). Its basic idea is to approximate an unknown function and its partial derivatives with respect to a spatial variable at any discrete point as the linear weighted sums of their values at all the discrete points chosen in the solution domain. To start with, we discretise the plate domain by N nodal lines parallel to x_2-axis, and designate the values of W, Ψ_1, Ψ_2, and F at an arbitrary nodal line $x_1 = x_{1i}$ $(i = 1, \ldots, N)$ as

$$W_i = W(x_{1i}, x_2), \qquad \Psi_{1i} = \Psi_1(x_{1i}, x_2), \qquad \Psi_{2i} = \Psi_2(x_{1i}, x_2), \qquad F_i = F(x_{1i}, x_2). \tag{23}$$

According to the differential quadrature rule, the unknown functions W, Ψ_1, Ψ_2, F, and their kth partial derivatives with respect to x_1 are expressed as

$$\{W, \Psi_1, \Psi_2, F\} = \sum_{j=1}^{N} l_j(x_1)\{W_j, \Psi_{1j}, \Psi_{2j}, F_j\}, \tag{24}$$

$$\frac{\partial^k}{\partial x_1^k}\{W, \Psi_1, \Psi_2, F\}\big|_{x_1 = x_{1i}} = \sum_{j=1}^{N} C_{ij}^{(k)}\{W_j, \Psi_{1j}, \Psi_{2j}, F_j\}, \tag{25}$$

where $l_i(x_1)$ is the Lagrange interpolation polynomial

$$l_i(x_1) = \frac{\prod_{j=1}^{N}(x_1 - x_{1j})}{(x_1 - x_{1i})\prod_{j=1, j\neq i}^{N}(x_{1i} - x_{1j})}, \tag{26}$$

and the weighting coefficients $C_{ij}^{(k)}$ can be obtained using the following recurrence formulas:

$$C_{ij}^{(1)} = \frac{\prod_{k=1, i\neq k}^{N}(x_{1i} - x_{1k})}{(x_{1i} - x_{1j})\prod_{k=1, j\neq k}^{N}(x_{1j} - x_{1k})} \quad (i, j = 1, 2, \ldots, N; \ i \neq j), \tag{27a}$$

$$C_{ij}^{(k)} = k\left(C_{ii}^{(k-1)}C_{ij}^{(1)} - \frac{C_{ij}^{(k-1)}}{(x_{1i}-x_{1j})}\right) \quad (i,j=1,2,\ldots,N;\ \ i\neq j;\ \ k\geqslant 2), \tag{27b}$$

$$C_{ii}^{(k)} = -\sum_{j=1;i\neq j}^{N} C_{ij}^{(k)} \quad (i=1,2,\ldots,N;\ \ k\geqslant 1). \tag{27c}$$

We further expand each of the unknown nodal functions W_i, Ψ_{1i}, Ψ_{2i}, and F_i as a linear sum as

$$(W_i,\Psi_{1i},\Psi_{2i},F_i) = \sum_{m=1}^{M}[a_{im}W_{im}, b_{im}\Psi_{1im}, c_{im}\Psi_{2im}, d_{im}F_{im}]\exp(i\omega t), \tag{28}$$

where $\omega = \Omega a^2\sqrt{I_1/D_{11}^*}$ is the dimensionless frequency parameter, Ω is the natural frequency, M is the truncated number of series, a_{im}, b_{im}, c_{im}, d_{im} are the unknown coefficients, and W_{im}, Ψ_{1im}, Ψ_{2im}, and F_{im} are the analytical functions that satisfy all of the boundary conditions (21a) or (21b), and take the following forms.

(1) For plates simply supported at both $x_2 = 0$, 1:

$$W_{im} = \sin(m\pi x_2), \tag{29a}$$

$$\Psi_{1im} = \sin(m\pi x_2), \tag{29b}$$

$$\Psi_{2im} = \cos(m\pi x_2), \tag{29c}$$

$$F_{im} = \sin\alpha_m x_2 - \sinh\alpha_m x_2 - \xi_m(\cos\alpha_m x_2 - \cosh\alpha_m x_2); \tag{29d}$$

(2) For plates clamped at both $x_2 = 0$, 1:

$$W_{im} = \sin\alpha_m x_2 - \sinh\alpha_m x_2 - \xi_m(\cos\alpha_m x_2 - \cosh\alpha_m x_2), \tag{30a}$$

$$\Psi_{1im} = \sin(m\pi x_2), \tag{30b}$$

$$\Psi_{2im} = \sin(m\pi x_2), \tag{30c}$$

$$F_{im} = \sin\alpha_m x_2 - \sinh\alpha_m x_2 - \xi_m(\cos\alpha_m x_2 - \cosh\alpha_m x_2); \tag{30d}$$

where $\xi_m = (\sin\alpha_m - \sinh\alpha_m)/(\cos\alpha_m - \cosh\alpha_m)$, $\alpha_m = (2m+1)\pi/2$.

Applying the relationships (24), (25), and (28) to the partial differential governing Eqs. (16)–(19) and the boundary conditions (20), and then employing Galerkin's procedure to minimize the interior residual by taking functions (29) or (30) as the weighting functions, gives a nonlinear eigensystem that consists of $4NM$ algebraic equations in matrix form of

$$\left(\begin{bmatrix} \mathbf{G}_{11} & \mathbf{G}_{12} & \mathbf{G}_{13} & \mathbf{G}_{14}+\mathbf{G}_{14}^* \\ \mathbf{G}_{21} & \mathbf{G}_{22} & \mathbf{G}_{23} & \mathbf{G}_{24} \\ \mathbf{G}_{31} & \mathbf{G}_{32} & \mathbf{G}_{33} & \mathbf{G}_{34} \\ \mathbf{G}_{41}+\mathbf{G}_{41}^* & \mathbf{G}_{42} & \mathbf{G}_{43} & \mathbf{G}_{44} \end{bmatrix} + \begin{bmatrix} \mathbf{0} & \mathbf{0} & \mathbf{0} & \mathbf{H}_{14}(\boldsymbol{\Delta}) \\ \mathbf{0} & \mathbf{0} & \mathbf{0} & \mathbf{0} \\ \mathbf{0} & \mathbf{0} & \mathbf{0} & \mathbf{0} \\ \mathbf{H}_{41}(\boldsymbol{\Delta}) & \mathbf{0} & \mathbf{0} & \mathbf{0} \end{bmatrix} - \omega^2 \begin{bmatrix} \mathbf{T}_{11} & \mathbf{T}_{12} & \mathbf{T}_{13} & \mathbf{0} \\ \mathbf{T}_{21} & \mathbf{T}_{22} & \mathbf{T}_{23} & \mathbf{0} \\ \mathbf{T}_{31} & \mathbf{T}_{32} & \mathbf{T}_{33} & \mathbf{0} \\ \mathbf{0} & \mathbf{0} & \mathbf{0} & \mathbf{0} \end{bmatrix}\right) \begin{Bmatrix} \mathbf{a} \\ \mathbf{b} \\ \mathbf{c} \\ \mathbf{d} \end{Bmatrix} = \begin{Bmatrix} \mathbf{0} \\ \mathbf{0} \\ \mathbf{0} \\ \mathbf{0} \end{Bmatrix} \tag{31}$$

in which the unknown vectors

$$\begin{aligned}
&\mathbf{\Delta} = [\mathbf{a}^{\mathrm{T}}, \mathbf{b}^{\mathrm{T}}, \mathbf{c}^{\mathrm{T}}, \mathbf{d}^{\mathrm{T}}]^{\mathrm{T}},\\
&\mathbf{a} = [a_{11}, \ldots, a_{1M}, \ldots, a_{iM}, \ldots, a_{NM}]^{\mathrm{T}}, \qquad \mathbf{b} = [b_{11}, \ldots, b_{1M}, \ldots, b_{iM}, \ldots, b_{NM}]^{\mathrm{T}},\\
&\mathbf{c} = [c_{11}, \ldots, c_{1M}, \ldots, c_{iM}, \ldots, c_{NM}]^{\mathrm{T}}, \qquad \mathbf{d} = [d_{11}, \ldots, d_{1M}, \ldots, d_{iM}, \ldots, d_{NM}]^{\mathrm{T}}.
\end{aligned} \tag{32}$$

$\mathbf{G}_{ij}$ $(i, j = 1, 2, 3, 4)$ and $\mathbf{T}_{ij}$ $(i, j = 1, 2, 3)$ are constant matrices, $\mathbf{G}^{*}_{14}$ and $\mathbf{G}^{*}_{41}$ are the matrices including the effect of the initial geometric imperfection, and $\mathbf{H}_{14}(\mathbf{\Delta})$ and $\mathbf{H}_{41}(\mathbf{\Delta})$ are the nonlinear matrices dependent on the unknown vector $\mathbf{\Delta}$.

After static condensation of Eq. (31), an iteration process is used to determine the nonlinear frequency with the following steps.

Step 1: Setting $\mathbf{\Delta} = \mathbf{0}$, a linear eigenvalue (fundamental frequency) and the associated eigenvector (vibration mode) are sought from Eq. (31). The eigenvector is then appropriately scaled up such that the maximum displacement is equal to a given vibration amplitude.

Step 2: Using the new eigenvector to calculate $\mathbf{H}_{14}(\mathbf{\Delta})$ and $\mathbf{H}_{41}(\mathbf{\Delta})$, a new eigenvalue and eigenvector are obtained from the updated eigensystem (31).

Step 3: The eigenvector is scaled up again and step 2 is repeated until the eigenvalue converges to a desired accuracy.

Obviously, linear vibration frequency can be solved from Eq. (31) as a limiting case by neglecting the nonlinear matrices.

4. Numerical results and discussion

4.1. Comparison results

Before proceeding to linear and nonlinear vibration analyses of imperfect FGM laminated plates, the nonlinear vibration of both simply supported isotropic and symmetric cross-ply laminated square plates with sine type initial geometric imperfection is solved as test examples to validate the present formulation and solution method.

For the isotropic plates ($v = 0.3$, $\eta = 0.2$, $a/h = 10, 20, 40$), present results with varying numbers of truncated series M and of the nodal lines N are compared in Table 2 with the analytical solutions of Singh et al. (1974) and Lin and Chen (1989). Close correlation is achieved. Some discrepancy is expected because their analyses were based on the FSDT and the in-plane displacement modes that they assumed were slightly different from the movable conditions that are considered in the present investigation.

Since the stiffness matrices of a symmetric cross-ply plate can be regarded as a limiting case of those of the laminated FGM plates and do not contain stretching-bending coupling elements, we further compare in Table 3 normalized frequencies $\omega_{\mathrm{NL}}/\omega_{\mathrm{L}}$ of both 90°/0°/90° and 0°/90°/0°/90°/0° symmetric cross-ply graphite/epoxy plates ($a/h = 10$, $\eta = 0.1$) with Bhimaraddi's parabolic shear deformation theory based results (Bhimaraddi, 1993) to validate the present analysis in composite laminates, where ω_{L} and ω_{NL} denote linear and nonlinear fundamental frequency of the imperfect plate, respectively. Excellent agreement is observed. The material constants used in this example are:

$$E_{11} = 181 \text{ GPa}, \quad E_{22} = 10.3 \text{ GPa}, \quad G_{12} = G_{13} = 7.17 \text{ GPa}, \quad G_{23} = 6.21 \text{ GPa}, v_{12} = 0.28.$$

In what follows, a symbolic notation will be used to indicate the out-of-plane boundary conditions. "SCSF", for example, refers to a laminated plate simply supported at $x_2 = 0$, 1, clamped at $x_1 = 0$, and free at $x_1 = 1$.

Table 2
Comparisons of nonlinear periods for simply supported imperfect isotropic square plates

a/h	W_c/h	Singh et al. (1974)	Lin and Chen (1989)	(N,M)			
				$(9,3)$	$(13,5)$	$(17,5)$	$(23,7)$
10	0.0	10.269	10.0353	8.1746	10.092	10.298	10.307
	0.1	10.24	9.98	8.1510	10.063	10.112	10.123
	0.2	10.15	9.87	8.1030	10.004	10.019	10.042
	0.4	9.67	9.23	7.6411	9.4001	9.4571	9.4602
	0.6	8.81	8.10	6.6197	8.1712	8.3370	8.3547
	0.8	7.85	6.97	5.5467	6.8478	6.9876	6.9916
	1.0	6.99	5.99	4.6636	5.7575	5.8750	5.8769
20	0.0	20.044	21.2688	18.285	21.017	21.446	21.468
	0.1	19.99	19.47	16.745	19.243	19.636	19.656
	0.2	19.81	19.30	16.583	19.060	19.443	19.469
	0.4	18.90	18.70	16.086	18.488	18.862	18.881
	0.6	17.27	15.89	13.647	15.684	16.001	16.023
	0.8	15.55	13.78	11.911	13.695	13.971	13.985
	1.0	13.77	12.02	10.429	11.987	12.232	12.244
40	0.0	39.840	42.2041	34.419	40.159	41.404	41.526
	0.1	39.74	38.73	32.309	37.700	38.866	38.983
	0.2	39.39	38.38	31.959	37.282	38.435	38.551
	0.4	37.59	35.94	29.931	34.925	36.006	36.114
	0.6	34.37	31.63	26.363	30.762	31.717	31.809
	0.8	30.75	27.44	22.970	26.803	27.632	27.715
	1.0	27.45	23.97	19.987	23.317	24.038	24.106

Table 3
Comparisons of normalized frequencies for simply supported imperfect symmetric cross-ply square plates

W_c/h	0°/90°/0°		0°/90°/0°/90°/0°	
	Present	Bhimaraddi (1993)	Present	Bhimaraddi (1993)
0.0	1.000	1.000	1.000	1.000
0.2	1.034	1.030	1.036	1.030
0.4	1.142	1.130	1.134	1.125
0.6	1.301	1.289	1.291	1.278
0.8	1.496	1.482	1.476	1.465
1.0	1.708	1.694	1.683	1.671
1.2	1.933	1.917	1.897	1.888

4.2. Linear vibration

In the following sections, it is assumed that the homogeneous substrate is made of stainless steel (SUS304) and the FGM layers are a mixture of silicon nitride and stainless steel, with temperature-dependent material constants

$$E = 348.43 \times (1 - 3.070 \times 10^{-4} \times T + 2.160 \times 10^{-7} \times T^2 - 8.946 \times 10^{-11} \times T^3)\ \text{GPa},$$
$$v = 0.24, \quad \alpha = 5.8723 \times 10^{-6} \times (1 + 9.095 \times 10^{-4} \times T)\ \text{K}^{-1}, \quad \rho = 2370\ \text{kg/m}^3$$

for silicon nitride and

$$E = 201.04 \times (1 + 3.079 \times 10^{-4} \times T - 6.534 \times 10^{-7} \times T^2)\ \text{GPa},$$
$$\nu = 0.3262 \times (1 - 2.002 \times 10^{-4} \times T + 3.797 \times 10^{-7} \times T^2),$$
$$\alpha = 12.33 \times 10^{-6} \times (1 + 8.086 \times 10^{-4} \times T)\ \text{K}^{-1}, \quad \rho = 8166\ \text{kg/m}^3$$

for stainless steel. The thickness ratio between the homogeneous substrate and the FGM layer is $h_c/h_F = 3$ and the side-to-thickness ratio is $a/h = 5$ except in Table 4 and Fig. 10. The values of I_1 and D_{11}^* of an isotropic steel plate with $a/h = 10$ at $T = 300$ K are selected to serve as the reference inertia I_0 and the reference stiffness D_0.

Tables 4–6 present the first 6 dimensionless linear frequencies $\omega = (\Omega a^2/\pi^2)\sqrt{I_0/D_0}$ for imperfect ($\eta = 0.2$) laminated square plates with three types of initial imperfections, together with those for perfect ($\eta = 0.0$) plates to demonstrate the effect of imperfection. The temperature is assumed to be $T = 300$ K.

Table 4 compares the linear results of simply supported, moderately thick ($a/h = 40$, 10) and thick ($a/h = 5$), FGM laminated ($n = 0.2$, 2.0, 10), and fully stainless steel plates with sine type imperfection. The linear frequency is the maximum for laminated plates of $n = 0.2$ and becomes smaller as n increases. This can be expected because the Young's modulus for silicon nitride is much greater than that for stainless steel, and the volume of silicon nitride declines when n increases. The linear frequency also decreases dramatically with increases in the side-to-thickness ratio a/h. The effect of the initial imperfections is to increase the vibration frequency. This effect, however, tends to be very weak as a/h increases to 40, which indicates that the geometric imperfection has much stronger influence on the vibration behavior of thicker plates.

Table 5 examines the effect of the location of local type imperfection on the linear frequencies of FGM laminated plates with different boundary supporting conditions (CCCC, SCSC, SSSS, CFCF, and SFSF). Given the same parameters, the plate with an imperfection locally centered at $x_1 = 0.5$ (Case L2) has higher frequencies than the one whose imperfection is deviated from the plate center and located at $x_1 = 0.25$ (Case L1). The fully clamped laminated plate has the highest linear frequencies among the plates considered.

Table 4
Linear frequency parameters for simply supported laminated square plates with sine type imperfection

a/h	Mode No.	Perfect				Imperfect			
		$n = 0.2$	$n = 2.0$	$n = 10$	SUS304	$n = 0.2$	$n = 2.0$	$n = 10$	SUS304
5	1	6.4388	5.6094	5.1983	4.9959	6.4636	5.6313	5.2192	5.0165
	2	13.902	12.183	11.338	10.922	13.917	12.196	11.350	10.934
	3	13.902	12.183	11.338	10.922	13.917	12.196	11.350	10.934
	4	19.937	17.546	16.374	15.796	19.948	17.555	16.383	15.805
	5	23.460	20.692	19.338	18.669	23.470	20.700	19.345	18.675
	6	23.460	20.692	19.338	18.669	23.470	20.700	19.345	18.675
10	1	2.5120	2.1792	2.0131	1.9310	2.5201	2.1865	2.0200	1.9379
	2	5.9606	5.1826	4.7958	4.6052	5.9649	5.1865	4.7995	4.6088
	3	5.9606	5.1827	4.7958	4.6052	5.9649	5.1865	4.7995	4.6088
	4	9.1059	7.9328	7.3515	7.0652	9.1087	7.9353	7.3539	7.0676
	5	11.066	9.6515	8.9519	8.6076	11.068	9.6535	8.9538	8.6094
	6	11.066	9.6515	8.9519	8.6076	11.068	9.6535	8.9538	8.6094
40	1	0.3256	0.2821	0.2602	0.2494	0.3266	0.2830	0.2611	0.2502
	2	0.8110	0.7026	0.6482	0.6214	0.8116	0.7031	0.6487	0.6219
	3	0.8110	0.7026	0.6482	0.6214	0.8116	0.7031	0.6487	0.6219
	4	1.2927	1.1201	1.0337	0.9909	1.2931	1.1204	1.0339	0.9912
	5	1.6120	1.3969	1.2892	1.2359	1.6122	1.3971	1.2894	1.2361
	6	1.6120	1.3969	1.2892	1.2359	1.6122	1.3971	1.2894	1.2361

Table 5
Linear frequency parameters for laminated square plates with localized imperfection

Plate type	Mode No.	Perfect			Case L1			Case L2		
		$n = 0.2$	$n = 2.0$	$n = 10$	$n = 0.2$	$n = 2.0$	$n = 10$	$n = 0.2$	$n = 2.0$	$n = 10$
CCCC	1	9.7131	8.5588	7.9958	9.7564	8.5971	8.0320	10.092	8.8980	8.3190
	2	16.866	14.930	13.996	16.974	15.025	14.085	16.875	14.938	14.003
	3	17.134	15.153	14.196	17.252	15.257	14.293	17.687	15.644	14.660
	4	22.916	20.307	19.047	23.200	20.555	19.280	22.961	20.346	19.083
	5	25.955	23.042	21.639	26.034	23.116	21.711	26.233	23.271	21.844
	6	26.759	23.683	22.172	26.940	23.834	22.306	27.591	24.410	22.854
SCSC	1	8.1526	7.1646	6.6825	8.1828	7.1911	6.7074	8.4531	7.4331	6.9382
	2	14.505	12.744	11.882	14.603	12.829	11.962	14.968	13.154	12.270
	3	16.171	14.302	13.401	16.246	14.368	13.462	16.176	14.306	13.405
	4	21.209	18.743	17.546	21.425	18.931	17.723	21.239	18.769	17.571
	5	23.708	20.925	19.565	23.881	21.076	19.706	24.362	21.502	20.109
	6	25.586	22.713	21.331	25.629	22.751	21.367	25.916	22.993	21.593
SSSS	1	6.4388	5.6094	5.1983	6.4914	5.6560	5.2428	6.7815	5.9143	5.4889
	2	13.902	12.183	11.338	13.984	12.255	11.406	13.907	12.188	11.342
	3	13.902	12.183	11.338	14.020	12.287	11.436	14.362	12.588	11.721
	4	19.937	17.546	16.374	20.158	17.739	16.556	19.965	17.570	16.397
	5	23.460	20.692	19.338	23.502	20.729	19.372	23.578	20.794	19.433
	6	23.460	20.692	19.338	23.663	20.869	19.503	24.253	21.384	19.986
CFCF	1	6.4849	5.6942	5.3055	6.5514	5.7531	5.3613	6.6632	5.8509	5.4531
	2	7.4929	6.5464	6.0836	7.5672	6.6122	6.1461	7.4978	6.5507	6.0877
	3	11.8946	10.349	9.5899	11.901	10.355	9.5958	12.216	10.632	9.8569
	4	14.8668	13.129	12.287	14.988	13.234	12.386	15.087	13.319	12.464
	5	16.2188	14.273	13.329	16.369	14.402	13.450	16.233	14.285	13.341
	6	20.132	17.550	16.281	20.198	17.608	16.335	20.139	17.555	16.287
SFSF	1	3.3602	2.9055	2.6787	3.4372	2.9741	2.7441	3.5759	3.0962	2.8596
	2	5.3156	4.5702	4.2029	5.3789	4.6265	4.2567	5.3184	4.5727	4.2053
	3	10.957	9.4870	8.7603	10.961	9.4907	8.7639	11.209	9.7085	8.9703
	4	11.499	10.032	9.3075	11.610	10.129	9.3977	11.696	10.202	9.4652
	5	13.308	11.580	10.728	13.431	11.686	10.827	13.319	11.588	10.736
	6	18.355	16.011	14.854	18.372	16.026	14.869	18.782	16.384	15.205

Table 6 investigates the effect of the global imperfection mode on the linear vibration of SSSS and CCCC FGM laminated plates. The half-wave number is taken to be the same along x_1- and x_2-axes, and is 3, 5, and 7 for Cases G1, G2, and G3, respectively. The linear frequency increases as the half-wave number increases. This effect is much more pronounced for SSSS laminated plates where a maximum of 31.2–32.5% gain in fundamental frequencies can be obtained with Case G3 imperfections.

The sensitivity of linear fundamental frequency to geometric imperfection is studied in Fig. 3 by comparing the sensitivity indicator S_ω of simply supported, FGM laminated square plates with sine type, Case G1, or Case L2 imperfections. Here, S_ω is calculated by

$$S_\omega = \frac{(\omega_{\text{imperfect}} - \omega_{\text{perfect}})}{\omega_{\text{perfect}}} \times 100\%, \tag{33}$$

where ω_{perfect} and $\omega_{\text{imperfect}}$ denote the dimensionless fundamental frequencies for perfect plates and imperfect plates, respectively. Among the imperfection modes under consideration, the linear frequency is

Table 6
Linear frequency parameters for laminated square plates with global imperfection

Imperfection	Mode No.	SSSS			CCCC		
		$n = 0.2$	$n = 2.0$	$n = 10$	$n = 0.2$	$n = 2.0$	$n = 10$
Perfect	1	6.4388	5.6094	5.1983	9.7131	8.5588	7.9958
	2	13.902	12.183	11.338	16.866	14.930	13.996
	3	13.902	12.183	11.338	17.134	15.153	14.196
	4	19.937	17.546	16.374	22.916	20.307	19.047
	5	23.460	20.692	19.338	25.955	23.042	21.639
	6	23.460	20.692	19.338	26.759	23.683	22.172
Case G1	1	6.5166	5.6785	5.2641	9.7606	8.6024	8.0381
	2	14.034	12.299	11.448	16.939	14.993	14.055
	3	14.067	12.328	11.475	17.202	15.212	14.250
	4	20.157	17.738	16.554	23.010	20.387	19.122
	5	23.987	21.150	19.766	26.605	23.604	22.162
	6	23.987	21.150	19.766	27.506	24.331	22.776
Case G2	1	6.5871	5.7414	5.3241	9.8215	8.6561	8.0887
	2	13.947	12.222	11.375	16.919	14.976	14.039
	3	13.983	12.255	11.406	17.339	15.334	14.367
	4	19.936	17.545	16.373	22.963	20.346	19.083
	5	23.654	20.861	19.496	26.913	23.818	22.296
	6	24.519	21.614	20.201	27.184	24.088	22.605
Case G3	1	8.4370	7.3813	6.8790	11.143	9.8274	9.2005
	2	14.760	12.939	12.052	17.998	15.939	14.957
	3	15.437	13.535	12.614	19.233	17.003	15.943
	4	20.796	18.300	17.083	24.548	21.752	20.416
	5	24.548	21.635	20.214	27.414	24.317	22.837
	6	25.262	22.265	20.812	29.328	25.920	24.261

most sensitive to localized imperfection, but is comparatively less sensitive to sine type imperfection. The results also confirm that the linear frequency increases steadily as the imperfection amplitude increases.

4.3. Nonlinear vibration

In this section, only nonlinear results for the fundamental vibration mode are presented, even though the analysis is also applicable to the non-fundamental modes. Unless otherwise specified, numerical results in the form of normalized frequency ω_{NL}/ω_0, given in Table 7 and Figs. 4–10 are for simply supported, FGM laminated square plates ($n = 0.2$, 10) at $T = 300$ K, where ω_{NL} is the nonlinear fundamental frequency of an imperfect plate and ω_0 is the linear fundamental frequency of its perfect counterpart, which is determined from the linear form of Eq. (31) by neglecting imperfection matrices $\mathbf{G}^*_{14}$, $\mathbf{G}^*_{41}$, and the nonlinear matrices $\mathbf{H}_{14}(\boldsymbol{\Delta})$ and $\mathbf{H}_{41}(\boldsymbol{\Delta})$.

The normalized frequencies of CCCC, SCSC, and SSSS imperfect laminated plates ($\eta = 0.2$) at various vibration amplitudes ($\overline{W}_c/h = 0.0$, 0.2, 0.4, 0.6, 0.8, 1.0) and with three types of initial imperfections (sine type, Case L2, and Case G1) are tabulated in Table 7. Note that the results at $\overline{W}_c/h = 0.0$ are virtually the frequency ratios between the linear fundamental frequency and ω_0. The normalized frequency rises with the increase of vibration amplitude, thus displaying the typical characteristic of the well-known "hard-spring" vibration behavior. The plate with Case L2 imperfection has the highest values of normalized frequency ω_{NL}/ω_0, but unlike the linear case discussed in Fig. 3, the values of ω_{NL}/ω_0 for the plate with sine type imperfections are greater than those with Case G1 imperfections.

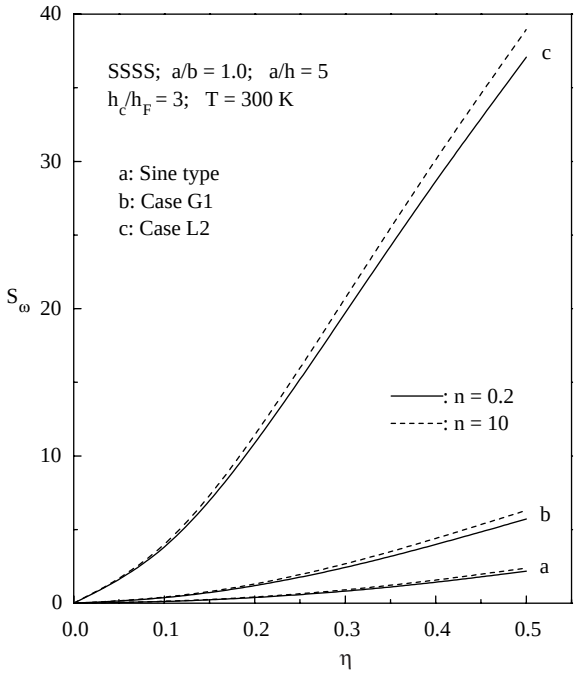

Fig. 3. Geometric imperfection sensitivity of linear fundamental frequency for simply supported laminated square plates.

Table 7
Normalized frequencies of laminated square plates with initial imperfection

Imperfection type	$\overline{W}_c/h$	CCCC			SSSS			SCSC		
		$n = 0.2$	$n = 2$	$n = 10$	$n = 0.2$	$n = 2$	$n = 10$	$n = 0.2$	$n = 2$	$n = 10$
Sine type	0.0	1.0029	1.0029	1.0030	1.0039	1.0040	1.0040	1.0030	1.0030	1.0031
	0.2	1.0224	1.0226	1.0231	1.0251	1.0256	1.0263	1.0216	1.0218	1.0222
	0.4	1.0577	1.0581	1.0593	1.0631	1.0644	1.0662	1.0551	1.0557	1.0569
	0.6	1.1048	1.1057	1.1076	1.1153	1.1175	1.1206	1.1003	1.1014	1.1036
	0.8	1.1607	1.1621	1.1650	1.1784	1.1818	1.1866	1.1539	1.1557	1.1592
	1.0	1.2238	1.2257	1.2296	1.2495	1.2542	1.2607	1.2140	1.2167	1.2213
Case L2	0.0	1.0956	1.0959	1.0977	1.1060	1.1084	1.1114	1.0940	1.0944	1.0962
	0.2	1.1430	1.1439	1.1464	1.1584	1.1618	1.1661	1.1411	1.1421	1.1450
	0.4	1.1953	1.1967	1.2001	1.2193	1.2238	1.2295	1.1928	1.1946	1.1986
	0.6	1.2531	1.2551	1.2592	1.2877	1.2933	1.3005	1.2488	1.2514	1.2564
	0.8	1.3177	1.3201	1.3251	1.3625	1.3691	1.3779	1.3097	1.3130	1.3191
	1.0	1.3906	1.3931	1.3989	1.4426	1.4503	1.4605	1.3760	1.3799	1.3870
Case G1	0.0	1.0089	1.0090	1.0093	1.0103	1.0105	1.0108	1.0117	1.0117	1.0119
	0.2	1.0218	1.0222	1.0230	1.0179	1.0183	1.0188	1.0221	1.0221	1.0226
	0.4	1.0462	1.0472	1.0487	1.0422	1.0431	1.0443	1.0437	1.0441	1.0451
	0.6	1.0809	1.0826	1.0848	1.0816	1.0833	1.0856	1.0750	1.0762	1.0780
	0.8	1.1257	1.1278	1.1309	1.1339	1.1366	1.1403	1.1155	1.1176	1.1205
	1.0	1.1812	1.1836	1.1875	1.1972	1.2011	1.2065	1.1653	1.1681	1.1723

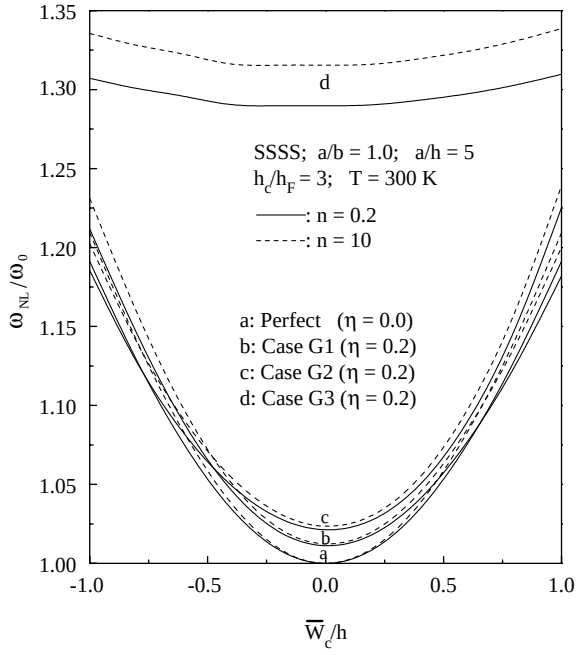

Fig. 4. Normalized frequencies versus vibration amplitude curves for simply supported laminated square plates with global imperfection.

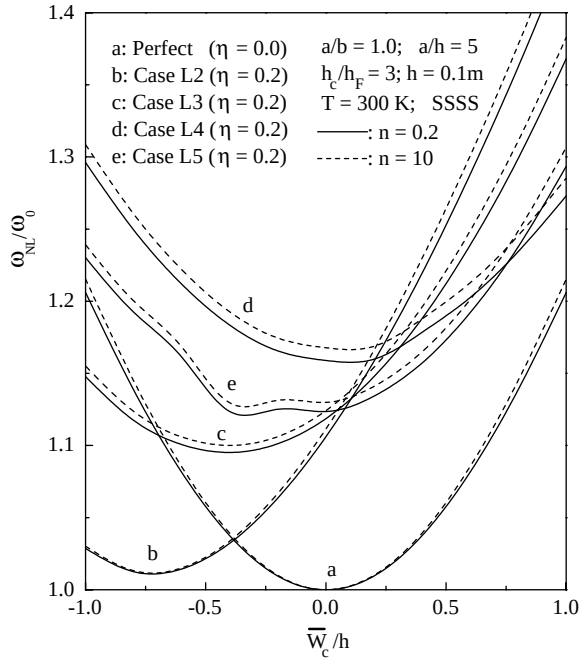

Fig. 5. Normalized frequencies versus vibration amplitude curves for simply supported laminated square plates with localized imperfection.

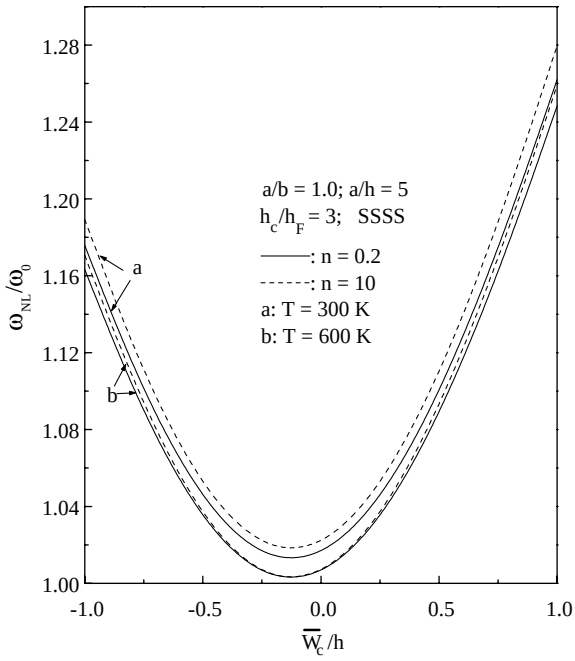

Fig. 6. Normalized frequencies versus vibration amplitude curves for simply supported laminated square plates at different temperatures.

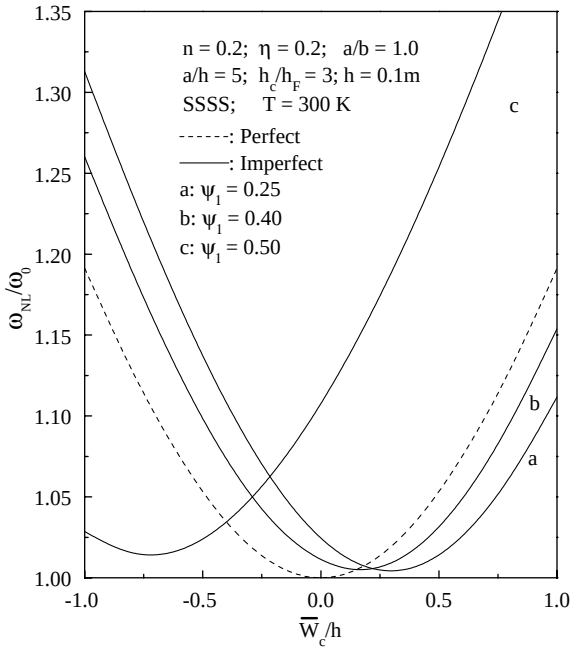

Fig. 7. Effect of imperfection location on the nonlinear vibration behavior of simply supported laminated square plates.

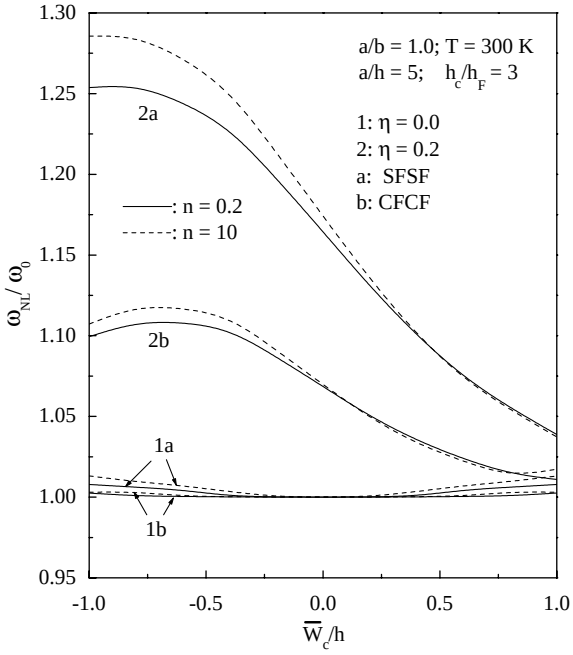

Fig. 8. Normalized frequencies versus vibration amplitude curves for SFSF and CFCF laminated square plates with localized imperfections (Case L2).

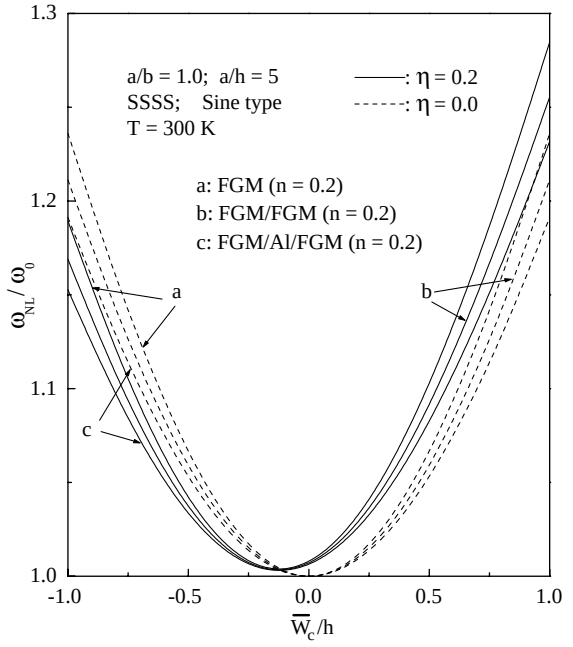

Fig. 9. Normalized frequencies versus vibration amplitude curves for simply supported laminated square plates with different material compositions.

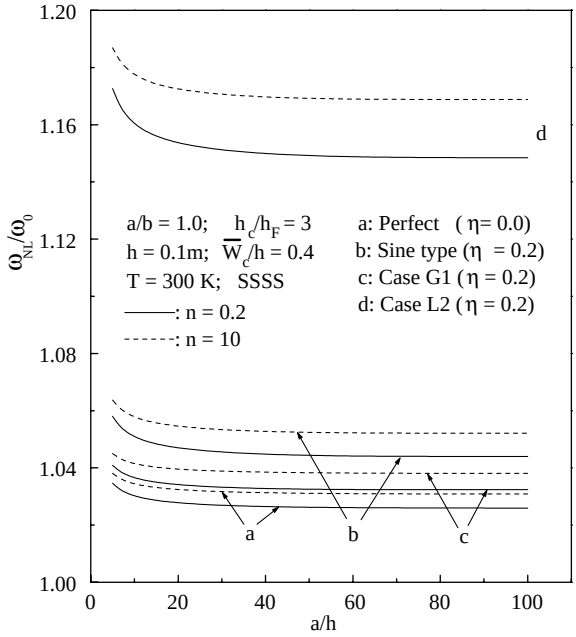

Fig. 10. Effect of side-to-thickness ratio on the nonlinear vibration behavior of simply supported laminated square plates with different initial imperfections.

Figs. 4 and 5 show the normalized frequency versus vibration amplitude curves for perfect and imperfect FGM laminated plates with global and localized imperfections. Curves a, which are for perfect plates, are exactly symmetric with $\overline{W}_c/h = 0.0$. For an imperfect plate, however, the minima, rising as the half-wave number increases, deviate from $\overline{W}_c/h = 0.0$, and the symmetry of the curves does not exist. Such a tendency is much more obvious in Fig. 5 for plates with localized imperfections.

Fig. 6 compare the normalized frequency versus vibration amplitude curves for FGM laminated plates at different temperatures ($T = 300$, 600 K). The curves become lower as temperature rises.

We next investigate the effect of imperfection location on the nonlinear vibration of FGM laminated plate. To this end, normalized frequency versus vibration amplitude curves with the center of Case L1 type imperfection located at $x_1 = 0.25$, 0.40, 0.50 are given in Fig. 7. As can be observed, the minima of the curves increase slightly and move further to the left-hand side as the imperfection location gets closer to the plate center.

Fig. 8 depicts the nonlinear vibration behavior of FGM laminated plates with free edges. The numerical results show that both CFCF and SFSF imperfect plates change to "soft-spring" vibration behavior from their inherent "hard-spring" behavior as the magnitude of central localized imperfection reaches a certain level ($\eta \geqslant 0.095$ for SFSF plates and $\eta \geqslant 0.055$ for CFCF plates). A similar phenomenon is found in all of the other examples involving free edges. This suggests that the vibration behavior of laminated plates containing free edges is very much dependent on the existence and amplitude of initial imperfection.

Fig. 9 gives the normalized frequency versus vibration amplitude curves for plates with sine type imperfection and having different material composition. Curves a, b, and c are for a fully FGM plate, a symmetrically laminated FGM/FGM plate, and an FGM/Al/FGM plate, respectively. The material profile of the first two plates can be characterized by ceramic volume fraction defined as

$$\text{FGM/FGM}: \quad V_c = (2X_3/h)^n, \quad X_3 \geqslant 0; \qquad V_c = (-2X_3/h)^n, \quad X_3 \leqslant 0; \tag{34a}$$

$$\text{Fully FGM}: \quad V_c = (0.5 + X_3/h)^n. \tag{34b}$$

The fully FGM plate has the highest ω_{NL}/ω_0 at negative vibration amplitudes, but has the lowest ω_{NL}/ω_0 at positive vibration amplitudes. In contrast, the normalized frequency of an FGM/Al/FGM laminated plate is the minimum when $\overline{W}_c/h < 0.0$, but becomes the maximum when $\overline{W}_c/h > 0.0$.

Fig. 10 examines the variation of ω_{NL}/ω_0 with side-to-thickness ratio a/h for simply supported laminated plates. For all plates, perfect and imperfect, ω_{NL}/ω_0 decreases with the increase of a/h, and tends to be a constant when $a/h \geqslant 20$.

5. Conclusions

The nonlinear vibration problems of imperfect, shear deformable, and FGM laminated rectangular plates are investigated in this paper by using Reddy's higher-order shear deformation plate theory and a semi-analytical approach. The influence of geometric imperfections, especially the localized type, is found to be highly significant on the vibration behavior of such laminated plate structures. The presence of localized imperfection at the plate center may significantly increase the linear frequencies and nonlinear normalized frequencies. Laminated plates with free edges may change their inherent "hard-spring" nonlinear vibration behavior to a "soft-spring" character when the imperfection magnitude reaches a certain level. The results also show that the vibration frequencies of thicker plates are much more sensitive to geometric imperfections than those of thinner plates.

Acknowledgements

The work described in this paper was supported by grants from the Australian Research Council (A00104534) and from the Research Grants Council of the Hong Kong Special Administrative Region, China (Project No. CityU 1024/01E). The authors are grateful for these financial supports.

References

Bellman, R.E., 1973. Methods of Nonlinear Analysis. Academic Press, New York.

Bert, C.W., Malik, M., 1996. Differential quadrature method in computational mechanics: A review. Applied Mechanics Review 49, 1–28.

Bert, C.W., Wang, X., Striz, A.G., 1993. Differential quadrature for static and free vibration analysis of anisotropic plates. International Journal of Solids and Structures 30, 1737–1744.

Bert, C.W., Jang, S.K., Striz, A.G., 1998. Two new approximate methods for analyzing free vibration of structural components. AIAA Journal 26, 612–618.

Bhimaraddi, A., 1993. Large amplitude vibrations of imperfect antisymmetric angle-ply laminated plates. Journal of Sound and Vibration 162, 457–470.

Bhimaraddi, A., Chandrashekhara, K., 1993. Nonlinear vibrations of heated antisymmetric angle-ply laminated plates. International Journal of Solids and Structures 30, 1255–1268.

Celep, Z., 1976. Free flexural vibration of initially imperfect thin plates with large elastic amplitudes. ZAMM 56, 423–428.

Celep, Z., 1980. Shear and rotatory inertia effects on the nonlinear vibration of the initially imperfect plates. Journal of Applied Mechanics ASME 47, 662–666.

Chen, L.W., Lin, C.C., 1992. Effects of geometric imperfections and large amplitudes on vibrations of an initially stressed Mindlin plate. Applied Acoustics 35, 265–282.

Chen, L.W., Yang, J.Y., 1993. Nonlinear vibration of antisymmetric imperfect angle-ply laminated plates. Composite Structures 23, 39–46.

He, X.Q., Ng, T.Y., Sivashanker, S., Liew, K.M., 2001. Active control of FGM plates with integrated piezoelectric sensors and actuators. International Journal of Solids and Structures 38, 1641–1655.

Hui, D., 1983. Large amplitude axisymmetric vibrations of geometrically imperfect circular plates. Journal of Sound and Vibration 91, 239–246.

Hui, D., 1985. Soft-spring nonlinear vibrations of antisymmetrically laminated rectangular plates. International Journal of Mechanical Sciences 27, 397–408.

Hui, D., Leissa, A.W., 1983. Effects of geometric imperfections on large amplitude vibrations of biaxially compressed rectangular flat plates. Journal of Applied Mechanics ASME 50, 750–756.

Ichikawa, K. (Ed.), 2000. Functionally Graded Materials in the 21st Century: A Workshop on Trends and Forecasts. Kluwer Academic Publishers, Japan.

Jang, S.K., Bert, C.W., Striz, A.G., 1989. Application of differential quadrature to static analysis of structural components. International Journal for Numerical Methods in Engineering 28, 561–577.

Kapania, R.K., Yang, T.Y., 1987. Buckling, postbuckling, and nonlinear vibrations of imperfect plates. AIAA Journal 25, 1338–1346.

Liew, K.M., Teo, T.M., Han, J.B., 2001. Three-dimensional static solutions of rectangular plates by variant differential quadrature method. International Journal of Mechanical Sciences 43, 1611–1628.

Liew, K.M., Yang, J., Kitipornchai, S., 2003. Postbuckling of the piezoelectric FGM plates subjected to thermo–electro–mechanical loading. International Journal of Solids and Structures 40, 3869–3892.

Lin, C.C., Chen, L.W., 1989. Large amplitude vibration of an initially imperfect moderately thick plate. Journal of Sound and Vibration 135, 213–224.

Markworth, A.J., Saunders, H., 1995. A model of structure optimization for a functionally graded material. Materials Letters 22, 103–107.

Noda, N., 1999. Thermal stresses in functionally graded materials. Journal of Thermal Stresses 22, 477–512.

Praveen, G.N., Reddy, J.N., 1998. Nonlinear transient thermoelastic analysis of functionally graded ceramic-metal plates. International Journal of Solids and Structures 35, 4457–4476.

Reddy, J.N., 1984. A refined nonlinear theory of plates with transverse shear deformation. International Journal of Solids and Structures 20, 881–896.

Reddy, J.N., 2000. Analysis of functionally graded plates. International Journal for Numerical Methods in Engineering 47, 663–684.

Reddy, J.N., Cheng, Z.Q., 2001. Three-dimensional solutions of smart functionally graded plates. Journal of Applied Mechanics ASME 68, 234–241.

Sathyamoorthy, M., 1987. Nonlinear vibration analysis of plates: A review and survey of current developments. Applied Mechanics Reviews 40, 1553–1561.

Shen, H.S., 2002a. Postbuckling analysis of axially loaded functionally graded cylindrical panels in thermal environments. International Journal of Solids and Structures 39, 5991–6010.

Shen, H.S., 2002b. Nonlinear bending response of functionally graded plates subjected to transverse loads and in thermal environments. International Journal of Mechanical Sciences 44, 561–584.

Shen, H.S., 2002c. Postbuckling analysis of axially-loaded functionally graded cylindrical shells in thermal environments. Composites Science and Technology 62, 977–987.

Shen, H.S., 2003. Postbuckling analysis of pressure-loaded functionally graded cylindrical shells in thermal environments. Engineering Structures 25, 487–497.

Shen, H.S., Leung, A.Y.T., 2003. Postbuckling of pressure-loaded functionally graded cylindrical panels in thermal environments. Journal of Engineering Mechanics ASCE 129, 414–425.

Singh, P.N., Sundararajan, V., Das, Y.C., 1974. Large amplitude vibration of some moderately thick structural elements. Journal of Sound and Vibration 36, 375–387.

Vel, S.S., Batra, R.C., 2002. Exact solution for thermoelastic deformations of functionally graded thick rectangular plates. AIAA Journal 40, 1421–1433.

Wadee, M.A., 2000. Effects of periodic and localized imperfections on struts on nonlinear foundations and compression sandwich panels. International Journal of Solids and Structures 37, 1191–1209.

Yamaki, N., Otomo, K., Chiba, M., 1983. Nonlinear vibrations of a clamped rectangular plate with initial deflection and initial edge displacement—Part 2: Experiment. Thin-walled Structures 1, 101–109.

Yang, J., Shen, H.S., 2002. Vibration characteristics and transient response of shear deformable functionally graded plates in thermal environment. Journal of Sound and Vibration 255, 579–602.

Yang, J., Shen, H.S., 2003a. Nonlinear bending analysis of shear deformable functionally graded plates subjected to thermo-mechanical loads under various boundary conditions. Composites Part B: Engineering 34, 103–115.

Yang, J., Shen, H.S., 2003b. Non-linear analysis of functionally graded plates under transverse and in-plane loads. International Journal of Non-Linear Mechanics 38, 467–482.

Yang, J., Shen, H.S., 2003c. Free vibration and parametric resonance of shear deformable functionally graded cylindrical panels. Journal of Sound and Vibration 261, 871–893.